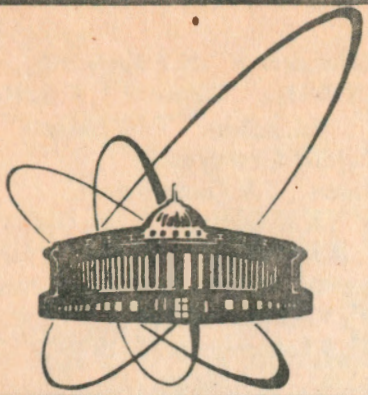

сообщения
объединенного
института
ядерных
исследований
дубна

E1-92-569

SILICON INDUCED INTERACTIONS WITH EMULSION AT 3.7 AND 14.6 AGeV

EMU01 — Collaboration

1992

Адамович М.И. и др.
E1-92-569

Взаимодействие ядер кремния с энергией 3,7 и 14,6 ГэВ на нуклон с ядрами фотоэмульсии

Сообщаются результаты исследования взаимодействий кремния-28 с ядрами фотоэмульсии при энергиях 3,7 и 14,6 ГэВ на нуклон. В нормированных переменных $n_s/\langle n_s \rangle$ наблюдается скейлинговое поведение. Плотность распределения однозарядных ливневых частиц по псевдобыстроте точно соответствует предельной фрагментации в собственной системе кремния-28.

Работа выполнена в Лаборатории высоких энергий ОИЯИ.

Сообщение Объединенного института ядерных исследований. Дубна, 1992

Adamovich M.I. et al.
E1-92-569

Silicon Induced Interactions with Emulsion at 3.7 and 14.6 AGeV

The new data on multiplicities and angular spectra of produced particles and target fragments from 14.6 AGeV silicion induced emulsion interactions are presented. Systematic comparison with Dubna silicon data at 3.7 AGeV is performed. Scaling is observed in the normalized variable $n_s/\langle n_s \rangle$ and in the dependence of the normalized multiplicities as a function of the charge flow in the forward direction for 14.6 and 3.7 AGeV. Limiting fragmentation behavior is observed in pseudorapidity density spectra of shower particles in the studied energy region. Multiplicities and angular spectra of low energetic target associated particles are weekly energy dependent in the studied energy region.

The investigation has been performed at the Laboratory of High Energies, JINR.

Communication of the Joint Institute for Nuclear Research. Dubna, 1992

M.I.Adamovich[13], M.M.Aggarwal[4], Yu.A.Alexandrov[13], N.P.Andreeva[1], Z.V.Anzon[1], R.Arora[4], F.A.Avetyan[20], S.K.Badya[18], E.Basova[17], K.B.Bhalla[7], A.Bhasin[8], V.S. Bhatia[4], V.G. Bogdanov[15], V.I.Bubnov[1], T.H. Burnett[16], X.Cai[19], I.Y.Chasnikov[1], L.P.Chernova[18], M.M.Chernyavsky[13], G.Z.Eligbaeva[1], L.E.Eremenko[1], A.S.Gaitinov[1], E.R.Ganssauge[12], S.Garpman[11], S.G.Gerassimov[13], J.Grote[16], K.G.Gulamov[18], S.K.Gupta[7], V.K.Gupta[8], H.H.Heckman[3], H.Huang[19], B.Jakobsson[11], B.Judek[14], L.Just[9], S.Kachroo[8], G.S.Kalyachkina[1], E.K.Kanygina[1], M.Karabova[6,9], G.L.Kaul[8], S.Kitroo[8], S.P.Kharlamov[13], S.A.Krasnov[6], V.Kumar[7], P.Lal[7], V.G.Larionova[13], V.N.Lepetan[1], L.S.Liu[18], S.Lokanathan[7], J.Lord[16], N.S.Lukicheva[18], S.B.Luo[10], T.N.Maksimkina[6], L.K.Mangotra[8], N.A.Marutyan[20], N.V.Maslennikova[13], I.S.Mittra[4], S.Mookerjee[7], H.Nasrulaeva[17], S.H.Nasyrov[17], V.S.Navotny[18], J.Nystrand[11], G.I.Orlova[13], I.Otterlund[11], H.S.Palsania[7], N.G.Peresadko[13], N.V.Petrov[17], V.A.Plyushchev[15], D.A.Qarshiev[17], W.Y.Qian[19], Y.M.Qin[10], R.Raniwala[7], S.Raniwala[7], N.K.Rao[8], V.M.Rappoport[13], J.T.Rhee[12], N.Saidkhanov[18], N.A.Salamanova[13], L.G.Sarkisova[20], V.R.Sarkisyan[20], G.S.Shabratova[6], T.I.Shakhova[1], S.N.Shpilev[18], D.Skelding[16], K.Soderstrom[11], Z.I.Solovjeva[15], E.Stenlund[11], E.L.Surin[18], L.N.Svechnikova[18], K.D.Tolstov[6], M.I.Tretyakova[13], T.P.Trofimova[17], U.Tuleeva[17], S.Vokal[6,9], H.Q.Wang[19], Z.Q.Weng[5], R.J.Wilkes[16], Y.L.Xia[5], G.F.Xu[2], D.H.Zhang[10], P.Y.Zheng[2], S.I.Zhokhova[18], D.C.Zhou[19]

[1]Alma Ata, Inst. of High Energy Physics, CIS
[2]Beijing, Academica Sinica, People's Republic of China
[3]Berkeley, Lawrence Berkeley Lab, USA
[4]Chandigarh, Panjab University, India
[5]Changsa, Hunan Education Inst., People's Republic of China
[6]Dubna, JINR, CIS
[7]Jaipur, University of Rajasthan, India
[8]Jammu, University of Jammu, India
[9]Kosice, Safarik University, Czechoslovakia
[10]Linfen,Shanxi Normal University, People's Republic of China
[11]Lund, University of Lund, Sweden
[12]Marburg, Philipps University, BRD
[13]Moscow, Lebedev Institute, CIS
[14]Ottawa, NRC, Canada
[15]St Petersburg, V.G.Khlopin Radium Institute, CIS
[16]Seattle, University of Washington, USA
[17]Tashkent, Institute of Nuclear Physics, CIS
[18]Tashkent, Physical-Technical Institute, CIS
[19]Wuhan, Hua-Zhong Normal Univ., People's Republic of China
[20]Yerevan, Physical Institute, CIS

1. Introduction

Recently, data on features of inelastic interactions of oxygen nuclei with emulsion at 14.6, 60 and 200 AGeV and sulphur nuclei with gold and emulsion at 200 AGeV were presented by the EMU01 collaboration (see [1] and references therein).

Here we report new experimental data on multiplicities and angular spectra of produced particles and target fragments obtained in ^{28}Si induced interactions with emulsion nuclei at 14.6 AGeV.

The experimental data are systematically compared with data obtained in the Dubna collaboration where inelastic interactions of ^{28}Si nuclei with emulsion nuclei were studied at 3.7 AGeV [2].

2. Experiment

In the experiment, layers of BR-2 photoemulsion with the dimensions 20cm x 10cm x 600 μm were irradiated horisontally by a silicon beam with an energy of 14.6 AGeV at BNL. The search of interactions was performed along the tracks of primary nuclei. The secondary particles were separated into s, g, b and f types in accordance with ordinary methodical emulsion criteria :

s-particles (shower) - singly charged particles with $\beta \geq 0.7$ outside the fragmentation cone;

g-particles (grey) - charged particles with a path in emulsion ≥ 3 mm, having $\beta<0.7$. These are mainly knock-out protons with kinetic energy 26 MeV ≤ T_{kin} < 400 MeV;

b-particles (black) - charged particles with a range in emulsion < 3 mm. These are mainly evaporation products from the remnant of the target nucleus;

f-particles - projectile spectator fragments, singly and multiple charged, emitted inside the fragmentation cone.

For all particles polar (θ) and azimuthal (Φ) emission angles were measured. All measurements of angles $\theta \leq 10$ deg were done relative to noninteracting beam tracks selected in the vicinity of the interaction vertex. Charge assignment for multiple charged f-particles was provided by delta-electron and/or gap density measurements.

Events which are due to electromagnetic dissociation and elastic scattering were excluded by the criterion that at least one shower particle should appear outside the fragmentation cone, which is 13 mrad at 14.6 AGeV [3]. After the subtraction of these events, 874 ^{28}Si-emulsion events remain out of a total sample of 955 events.

A systematic comparison was performed with 1209 inelastic ^{28}Si- emulsion events at 3.7 AGeV [2] which were obtained from a total sample of 1322 events after subtracting electromagnetic and elastic events (using a fragmentation cone of 44 mrad).

3. Multiplicity distributions

Fig.1 presents the multiplicity distributions of shower particles for 14.6 and 3.7 AGeV, respectively. As can be seen in the figure the observed tails of the distributions extend up to 140 and 70 shower particles for the two incident energies, respectively.

The distributions of normalized shower particle multiplicity $n_s/\langle n_s \rangle$ for 14.6 and 3.7 AGeV are shown in figure 2. The striking observation is that the data fall on the same universal curve, as do the oxygen induced emulsion interactions at 200, 60 and 14.6 AGeV [3]. In this paper it was pointed out that this scaling is a consequence of the nuclear geometry, which is energy independent, and reflects the distribution of the number of participating nucleons from the two nuclei.

The next figures show the features in the target fragmentation region. The distributions of the number of grey particles (i.e.recoil target protons) and black particles (i.e. slow target fragments) at two energies are presented at figs.3 and 4,

respectively. The correlations of multiplicities $\langle n_b \rangle = f(n_g)$ and $\langle n_g \rangle = f(n_b)$ are given in Figs.5 and 6, respectively.

One can see that the n_g- and n_b- spectra are approximately energy independent. This is better fulfilled for slower, i.e. black target fragments. Some difference is seen on the tails of these distributions, where an enhanced tail is seen for lower primary energy.

The mean number of evaporated b-particles increases linearly with impact parameter as measured by the number of g-particles, i.e. recoil target protons, up the values of $n_g \cong 10$. The following saturation at higher values of n_g can be explained by the conservation of the nucleon number in the target nucleus, i.e. by the limited mass of the target nucleus.
Week dependence on the primary silicon energy is seen. The analogical behaviour is seen in the case of $\langle n_g \rangle = f(n_b)$ correlation, where in the plateau region some excess in recoil protons production is observed at 3.7 AGeV.

4. Average multiplicities and their variation with centrality.

Table 1 presents the average multiplicities for secondary particles of different types in ^{28}Si induced emulsion collisions at 14.6 AGeV as well as the corresponding values at 3.7 AGeV. We point out the high increase in the number of produced particles (shower particles) in contrast to the conservativity in the number of target fragments.

The difference in the mean numbers of g-particles 6.9 ± 0.2 and 5.4 ± 0.2 may be explained by the fact that recoil protons from the hard part of the momentum spectrum turn into s-particles when primary energy increases.

Table 2 presents the average multiplicities of shower particles and the dispersions of the n_s- distributions for various groups of events, characterized by the numbers of target fragments N_h, where $N_h = n_g + n_b$.

In the groups with $N_h \leq 7$ there are interactions with hydrogen, light nuclei (C, N, O) and "peripheral" interactions with heavy nuclei (Br, Ag) . The groups with $N_h \geq 8$ are formed by events which occured with the heavy target components of emulsion, exclusivly.

We point out that the number of produced particles increases

rapidly with the desintegration of the target nucleus, which is more strikingly seen at 14.6 AGeV.

It can be understand in a geometrical picture, where in a non-peripheral (or central) collisions of two nuclei, which are characterized by the high number of h-particles, relatively large parts of target nuclei are involved in the interaction and so a large number of shower particles are created.

An interest is to performe the analysis of the multiplicity dependences on a quantity Q , which measures the total charge of noninteracting projectile fragments, $Q = n_i Z_i$, where n_i is the number of fragments with charge $Z_i \geq 1$ in any given event.

The distributions of events with a given value of Q for both incident energies are presented in fig.7 . The comparison shows that the Q - distributions seem to be independent of incident energy.

The value of Q characterizes the volume of the nonoverlapping part of the projectile nucleus. Thus this quantity enables us to evaluate the number $n_{int} \cong (Z_p - Q) A_p / Z_p$ of primary nucleons which have interacted with the target nucleus, Z_p and A_p are the atomic and mass numbers of the projectile nucleus.

Thus the distribution of the number of participating nucleons from the primary nucleus is energy independent within the statistical uncertaintes of our experiments pointing to the importance of the nuclear geometry.

Fig.8 shows the distributions of another frequently used quantity $Q_{zd} = Q + n_s (\theta_s \leq \theta_{zd})$, where the cut angle θ_{zd} corresponds the values of 39 and 133 mrad at 14.6 and 3.7 AGeV, respectively (for definition of θ_{zd} see e.g.[3]). We see that Q_{zd} distributions are independent of incident energy, the same result as obtained for oxygen induced emulsion interactions, but for higher energies.

Figure 9 shows the dependence of the average multiplicity of produced particles and target fragments, fast and slow, on the value of Q, which may be used for classification of nucleus - nucleus interactions according to the degree of centrality . It seems reasonable to treat interactions with small Q as central ones and those with large Q as peripheral ones, with a large impact parameter [4]. One can see that the multiplicities of shower particles and fast target fragments increase rapidly with

increasing centrality. This dependence is weeker in the case of b-particles, which consist of essentialy only target spectator fragments. The lower Q, the more significant difference in shower particle production at 14.6 and 3.7 A GeV, not seen so strong in the case of target fragments. Moreover the dependence of $\langle n_b \rangle$ on Q shows an indication of saturation with decreasing Q.

In fig.10a we show the "normalized" quantity $\langle n_s \rangle_Q / \langle n_s \rangle$ as a function of Q. We point out that the data for the two incident energies seems to fall on a universal curve. The dependence of $\langle n_s \rangle_{Q_{zd}} / \langle n_s \rangle$ on the value of Q_{zd} (fig.10b) shows also perfectly universal behavior at 14.6 and 3.7 AGeV primary energies.

The same scaling with respect to incident energies in terms of normalized variables $n_s / \langle n_s \rangle$ and $\langle n_s \rangle_{Q_{zd}} / \langle n_s \rangle$ was obtained recently in the EMU01 study of 14.6, 60 and 200 AGeV oxygen data [3].

5. Angular distributions

The pseudorapidity density distributions ($\rho = 1/N_{ev} . dN_{tr}/d\eta$) of produced particles and single charged projectile fragments (s'-particles) for the minimum bias samples at two different energies are shown in figs.11 and 12. In fig.11 the comparison is made in the target rest frame and in fig.12 in the projectile rest frame, where η_p is given by $\eta_p \cong y_p + 0.08$ [3], y_p is the rapidity of the projectile.

We see perfectly limiting fragmentation behavior in the projectile rest frame in studying energy region. The difference between two spectra in the target rest frame may be explained by the fact that at Dubna energy the multiplicity of relativistic pions is less than in BNL region and so the relative yield of hard protons is higher and the pseudorapidity spectrum is shifted to the right.

When soft protons are included in analysis, fig. 13 shows scaling in target rest frame for η-spectra of s- and g-particles.

The pseudorapidity density spectra for different centrality cuts are presented in fig.14 for the case of ^{28}Si-induced interactions in emulsion at 14.6 AGeV only. We point out that the densities of produced particles in the central region reach for central events high values about 30-35 particles per unit pseudorapidity interval in contrast to the case of lower primary energy of silicon nuclei (not presented here).

The angular spectra of grey particles at the two energies are shown in Fig.15 together with a fit (solid line) from proton induced emulsion interactions [5,6].

A fit to the silicon data with an exponential form gives $e^{1.06\cos\theta}$ and $e^{1.30\cos\theta}$ at 14.6 and 3.7 AGeV, respectively. Thus the nuclear data shows a deeper dependence on the emission angle of grey particle. Our results are in accordance with previously published carbon induced emulsion data at Dubna energy [7] where recoil protons angular spectrum was described by $e^{1.15\cos\theta}$.

Fig.16 deals with the angular distributions of black particles. The spectra are similar within the statistical uncertaintes of our experiments although the drastic drop at large angles ($\cos\theta < -0.5$) observed at 14.6 AGeV [8] is not not seen at lower energy data.

6. Conclusions

In our first study of multiplicities and angular spectra of produced particles and target fragments in silicon induced emulsion interactions at 14.6 AGeV a systematic comparison with Dubna emulsion silicon data at 3.7 AGeV was performed.

Scaling was observed in the normalized variable $n_s/\langle n_s\rangle$ for 14.6 and 3.7 AGeV. The dependence of the normalized multiplicities $\langle n_s\rangle_Q / \langle n_s\rangle$ on the charge flow in the forward direction Q seems to be independent of incident energies.

The pseudorapidity density distributions of relativistic singly charged particles in silicon induced emulsion interactions at 14.6 and 3.7 AGeV show perfectly limiting fragmentation behavior in the projectile rest frame which is less seeing in the target rest frame.

No energy dependence has been obtained in the multiplicity spectra of the target - associated particles. On the other hand we point out the week energy dependence in the multiplicity correlations between target fragments and in their angular spectra. The increase of the yield of the target fragments in the central collisions of ^{28}Si with emulsion at 3.7 AGeV, more striking for the fast target fragments has been observed.

Table 1. The characteristics of the samples used.

	Energy in AGeV	
	3,7	I4.6
n_s	I2.9 ± 0.4	28.8 ± I.0
n_g	6.9 ± 0.2	5.4 ± 0.2
n_b	4.7 ± 0.I	4.3 ± 0.I
Nevents	I209	874

Table 2. The characteristics of the shower particle multiplicity distributions at 14.6 and 3.7 AGeV incident silicon energy as a function of N_h.

N_h		Energy in AGeV	
		3.7	I4.7
0 - I	n_s	3.9 ± 0.3	8.8 ± 0.7
		3.87	I0.03
	Nev	2I7	I98
2 - 7	n_s	8.0 ± 0.3	I6.8 ± 0.8
		6.42	I3.90
	Nev	446	3I5
8 - I5	n_s	I0.I ± 0.6	27.7 ± 2.0
		7.56	2I.78
	Nev	I80	II7
I6 - 27	n_s	20.7 ± 0.9	55.8 ± 2.2
		I2.7	29.09
	Nev	I93	I8I
28	n_s	30.9 ± I.0	76.I ± 3.4
		I2.7	27.22
	Nev	I73	63

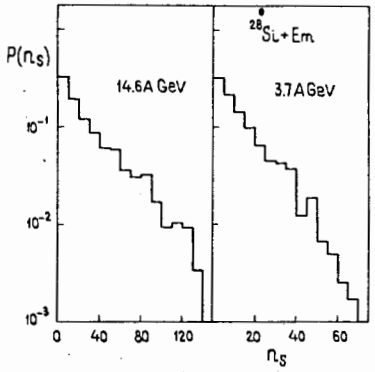

Fig.1. The multiplicity distributions of shower particles for 14.6 AGeV and 3.7 AGeV incident silicon energy.

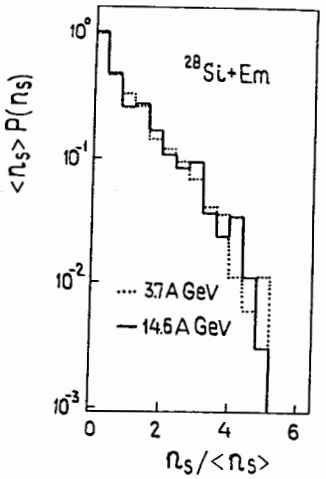

Fig.2. The distribution of normalized s-particle multiplicity for 14.6 and 3.7 AGeV incident silicon energy.

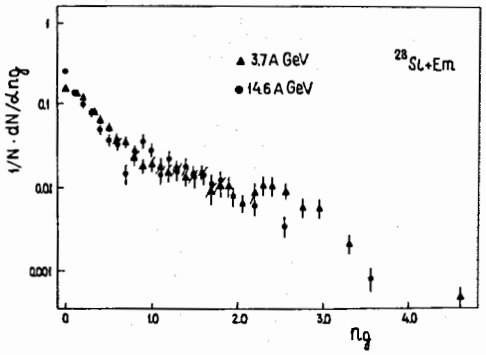

Fig.3. The multiplicity distributions of grey prongs in silicon induced interactions with emulsion at 14.6 and 3.7 AGeV.

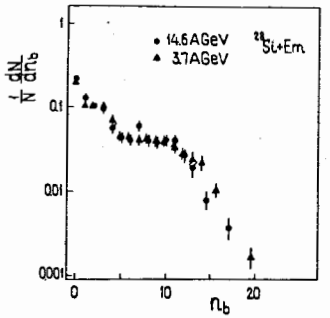

Fig.4. The multiplicity distributions of black prongs in silicon induced interactions with emulsion at 14.6 and 3.7 AGeV.

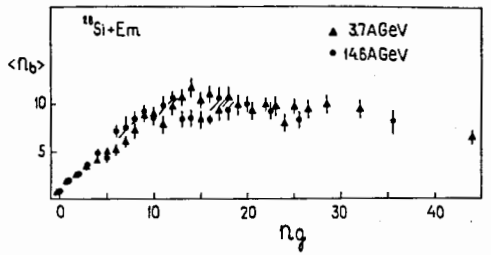

Fig.5. The average number of black prongs versus n_g at 14.6 and 3.7 AGeV incident silicon energy.

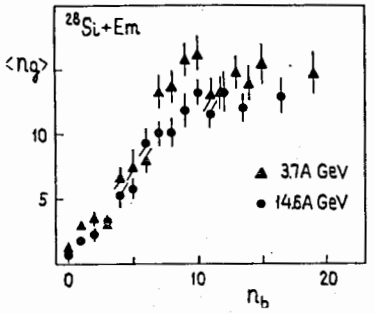

Fig.6. The average number of grey prongs versus n_b at 14.6 and 3.7 AGeV incident silicon energy.

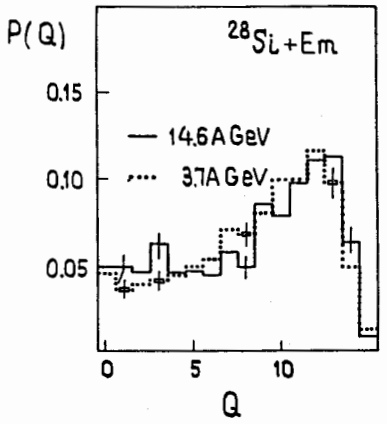

Fig.7. The distribution of events with a given value of Q for 14.6 and 3.7 AGeV.

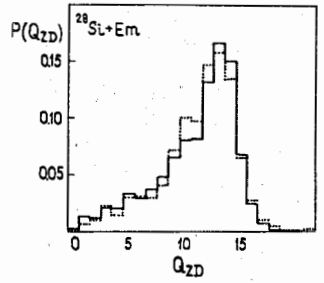

Fig.8. The distribution of events with a given value of Q_{zd} for 14.6 and 3.7 AGeV.

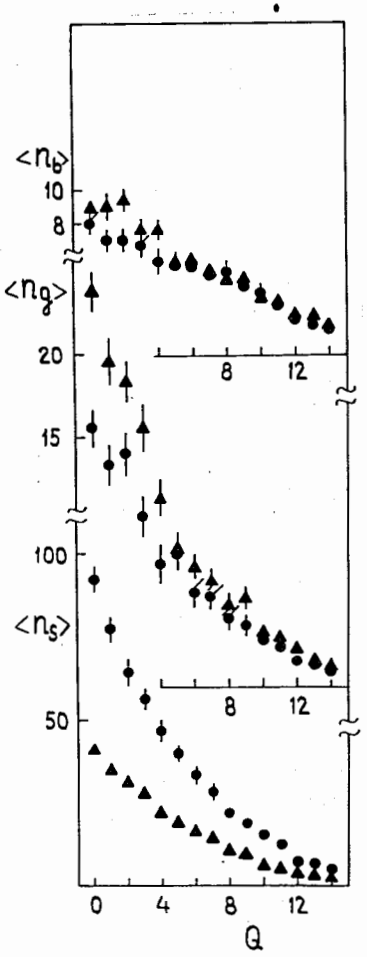

Fig.9. The average multiplicity of shower, grey and black particles as a function of Q for 14.6 and 3.7 AGeV.

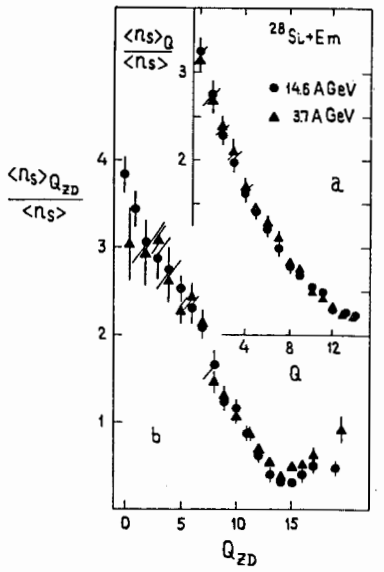

Fig.10. The normalized average multiplicity $\langle n_s \rangle_Q$ / $\langle n_s \rangle$ as a function of Q (a) and Q_{zd} (b) for 14.6 and 3.7 AGeV.

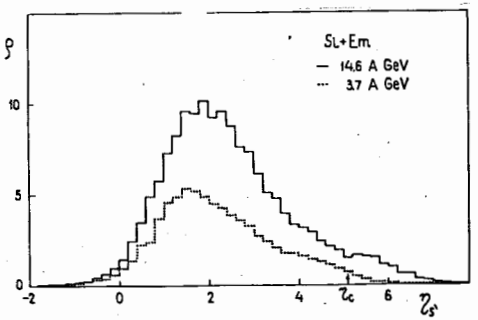

Fig.11. The pseudorapidity density distributions of shower particles and single charged projectile fragments in the target rest frame in silicon induced interactions with emulsion at 14.6 and 3.7 AGeV .

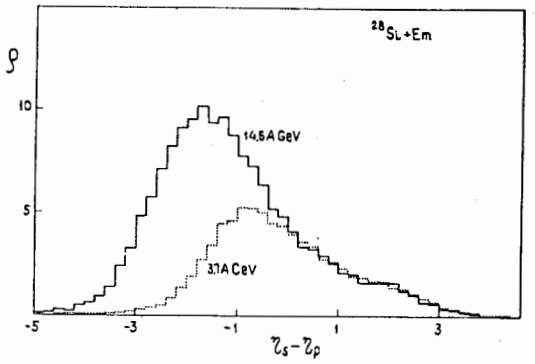

Fig.12. The pseudorapidity density distributions of shower particles and single charged projectile fragments in the projectile rest frame in silicon induced interactions with emulsion at 14.6 and 3.7 AGeV .

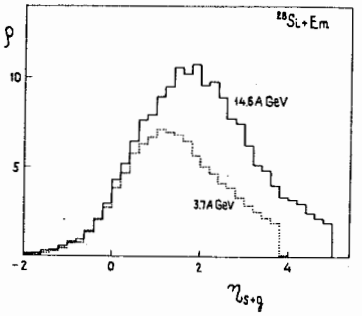

Fig.13. The pseudorapidity distributions of s- and g-particles in the target rest frame for 14.6 and 3.7 AGeV incident silicon energy.

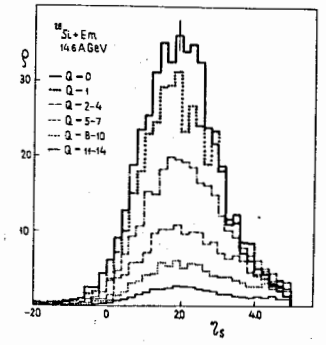

Fig.14. The pseudorapidity density spectra of shower particles for 14.6 AGeV incident silicon energy as a function of Q.

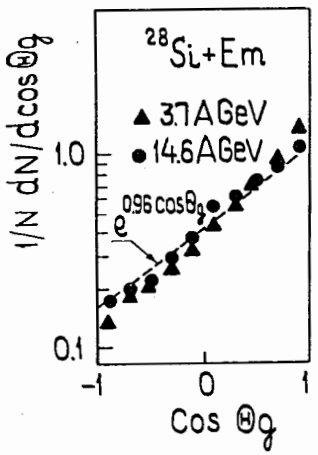

Fig.15. The angular spectra of grey prongs at 14.6 and 3.7 AGeV incident silicon energy compared with proton induced emulsion interactions (dashed line).

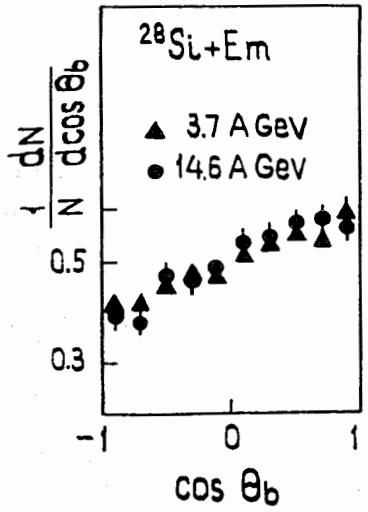

Fig.16. The angular spectra of black prongs at 14.6 and 3.7 AGeV incident silicon energy.

References :

1. E.Stenlund et al.,Lund preprint,LUIP 9004,Lund,1990.
Proc. Hipags Workshop, BNL, March 1990.
2. B.U.Ameeva et al.,Sov.J.Nucl.Phys.,51(1990)1047;
3. M.I.Adamovich et al.,Phys.Lett.,B223(1989)262.
4. M.I.Adamovich et al.,Dubna preprint,E1-10838,Dubna,1977.
5. B.Slowinski,E.Mulas,S.Vokal,Dubna commun.,P1-83-202,Dubna,1983.
6. I.Otterlund et al.,Nucl.Phys.,B142(1978)445.
7. S.Vokal,M.Shumbera,Sov.J.Nucl.Phys.,39(1984)1474.
8. M.I.Adamovich et al.,Lund preprint,LUIP 9103,Lund,1991.

Received by Publishing Department
on December 29, 1992.